

Automatic Detection of Microaneurysms in Fundus Images

Jesús Eduardo Ochoa Astorga, Kyoto Institute of Technology, Japan

Linni Wang, Tianjin Medical University Eye Hospital, China

Shuhei Yamada, Kyoto Institute of Technology, Japan

Yusuke Fujiwara, Kyoto Institute of Technology, Japan

Weiwei Du, Kyoto Institute of Technology, Japan*

Yahui Peng, Beijing Jiaotong University, China

ABSTRACT

Early detection and treatment of diabetic retinopathy can delay blindness and improve quality of life for diabetic patients. It is difficult to detect early symptoms of diabetic retinopathy, which is presented by few microaneurysms in fundus images. This study proposes an algorithm to detect microaneurysms in fundus images automatically. The proposal includes microaneurysms segmentation by U-Net model and their false positives removal by ResNet model. The effectiveness of the proposal is evaluated with the public database IDRiD and E-optha by the area under precision recall curve (AUPR). 90% of microaneurysms can be detected at early stages of diabetic retinopathy. This proposal outperforms previous methods based in AUPR evaluation.

KEYWORDS

Computer Aided Diagnosis, Deep Learning, Diabetic Retinopathy, Retinal Disease

INTRODUCTION

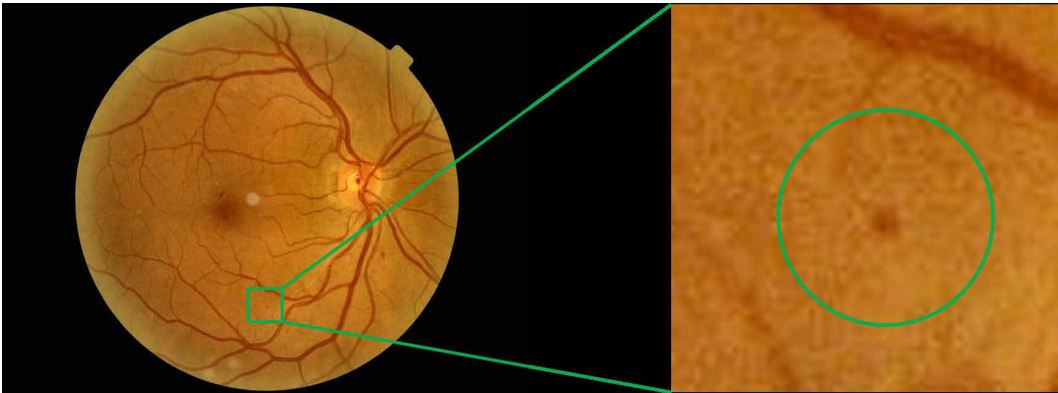
Diabetic retinopathy (DR) is a complication of diabetes mellitus that may occur if the latter is left untreated. During DR, retina undergoes a group of lesions that gradually deteriorate it, being this condition the most frequent cause of blindness worldwide in individuals aged 20–74 years (Mahendran & Dhanasekaran, 2015). Therefore, detection in early stages is particularly important, as it helps ophthalmologists to administer appropriate treatments that improve patients health condition and hence protecting them from an irreversible damage, such as vision loss. The most common method employed by physicians for detecting DR is through the analysis of fundus photography, in which the disease shows up as hemorrhages, exudations and microaneurysms (MAs), being the last one the most important clinical finding in the diagnosis of DR, as they are the first lesion that appears during the early stages (Selcuk & Alkan, 2019; Sarhan et al., 2019). MAs appear as small red dots, and the main complication in their adequate detection is their similarity to vessel fragments (Bhatia et al., 2016). An example of MA in fundus image is shown in Figure 1.

DOI: 10.4018/IJSI.315658

*Corresponding Author

This article published as an Open Access article distributed under the terms of the Creative Commons Attribution License (<http://creativecommons.org/licenses/by/4.0/>) which permits unrestricted use, distribution, and production in any medium, provided the author of the original work and original publication source are properly credited.

Figure 1. Fundus image with presence of a MA



In common practice, the judgment by physicians is done visually based only on their experience, meaning that this process is time consuming, subjective and, as a result, this gives rise to differences in judgment. Besides, concerning the number of MAs found in fundus during the assessment, this helps to determine the severity of DR, however, the number may turn to be irrelevant, as the sole presence of one single MA is indicative of DR. Due to this, it is essential for computer-aided diagnosis (CAD) systems to detect MAs regardless their position or the amount of these. Inspired in avoiding subjectivity, speeding up the assessment process and increasing the sensitivity of fundus evaluation, several proposals have been suggested for detection and segmentation of MAs in fundus images.

BACKGROUND

Kumar and Kumar (2018) developed a method based on diverse image transformations that include principal component analysis (PCA) and contrast enhancement as pre-processing stage, and subsequently different regions of fundus photography are discarded, namely, exudates, blood vessels, optic disc and fovea, to remain only MAs, which are used to extract features and pass them to a support vector machine (SVM) for DR detection. Similarly, Joshi and Karule (2020) performed MAs detection by implementing image reconstruction over a pre-processed grayscale image obtained from green channel of RGB fundus image. Then, blood vessels and bright artifacts are removed and after connected component analysis, candidate MAs are detected. Lastly, after feature extraction, MAs are detected. The limitation of these approaches lies in the similarity of MAs with blood vessels, and for this reason, it is crucial a satisfactory blood vessels network segmentation. Furthermore, methods primarily based on image processing techniques are highly sensitive to non-uniform illumination occurred during fundus image acquisition, where the geometry of the eye causes internal reflection that contributes to the presence of shading artifacts (Manohar & Singh, 2018). For this reason, other researchers make the most of deep learning to achieve this task.

Jiang et al. (2019) proposed a deep learning lesion-based method for DR disease classification, in which MAs are one of the contemplated lesions. In this study three different deep learning models are used for classification, namely, Inception V3, ResNet152 and Inception-ResNet-V2. Each of these showed favorable results in classification, however, even if separately each model performed satisfactorily, the weights and bias of each fall into local minimums. Thereby, considering the results obtained from each model, a global minimum is searched by using the Adaboost algorithm to create a more robust classifier by associating each individual model. Likewise, Eftekhari et al. (2019) used more than one single deep learning model. In their proposal, fundus pre-processed image is divided in patches that are passed to a basic convolutional neural network (CNN) that returns a probability

map, specifying the likelihood for each pixel to be a MA which is thresholded with a fixed value. As the obtained result is noisy, a second CNN operates decreasing the false-positive rate, therefore, the threshold probability map is re-evaluated by a second CNN to generate a final probability map for MAs.

This paper proposes an algorithm that takes advantage of pre-existing deep learning models, namely U-Net (Ronneberger et al., 2015) and ResNet (He et al., 2016), to tackle MAs segmentation. As Jiang et al. (2019) demonstrated, popular models have a suitable performance in MAs detection, showing an accuracy over 0.86 and an AUC over 0.93 in lesions detection. In the IDRiD: Diabetic Retinopathy-Segmentation and Grading Challenge (Porwal et al., 2020), a pixel-by-pixel segmentation was used. Yet, the results included many false positives. Therefore, there are still many problems in the accurate detection. Thereby, rather than finding candidate regions (Miyashita et al. 2018) or a probability map (Jiang et al., 2019; Eftekhari et al., 2019), this work aims at generating an accurate MAs segmentation. Instead of using simultaneously the two models, firstly, inspired in the research of Eftekhari et al. (2019), U-Net performs MAs detection and afterwards, ResNet removes false-positives from primary result.

This paper is established as follows. After introduction, the proposed method is explained. Next, experimental results are shown and conclusion and future work are discussed.

PROPOSED METHOD

In this section, the concept of the proposed method is introduced: Description of the algorithm flowchart, Portrayal of the preprocessing stage, MAs segmentation with U-Net and False-positive removal with Res-Net.

Flowchart

Flowchart shown in Figure 2 provides a brief description of the proposed method. The input is a color fundus image. Firstly, gamma correction is applied to the input image for contrast manipulation. Then, contrast limited adaptive histogram equalization algorithm (CLAHE) (Pizer et al., 1987) is employed for emphasizing more the difference between MAs and background. Once MAs are emphasized, U-Net (Ronneberger et al., 2015) receives patch images as input and detects MAs on them. Result obtained from U-Net includes several false positives, therefore ResNet (He et al., 2016) is used as a classifier to determine, for each patch image containing MAs according to U-Net, whether it contains MAs or not. The proposed method is explained more in detail in the next sections.

Preprocessing

The purpose of this phase is improving the quality of fundus image by enhancing the contrast between MAs and the background. Fundus images tend to be dark, and MAs are darker than background. For this reason, it is difficult to differentiate MAs from background. To improve brightness and contrast between MAs and background, firstly gamma correction is applied, which is described by the equation:

$$y = 255 \left(\frac{x}{255} \right)^{1/\gamma}$$

where x is the original pixel, y is the resultant pixel and γ is the gamma correction value. For the proposed method, γ is set to $\gamma = 1.5$. This value was obtained empirically. The result is a brighter image where it is easier to differentiate MAs and background. After gamma correction, CLAHE is applied, which makes histogram flattening to regions of the image. In this work, these regions are set to an area of 8×8 pixels and, for excluding areas other than fundus, a mask is used in this process.

Figure 2. Flowchart of proposed method

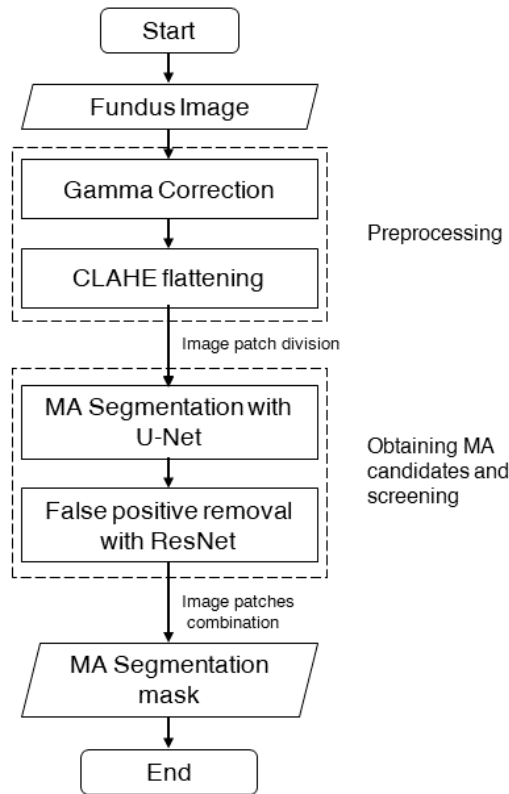


Figure 3 shows the result of gamma correction and CLAHE algorithm. The result is an image where details such as the MAs and blood vessels are more perceptible.

MAs Segmentation

For MAs segmentation the authors adopted U-Net architecture, a kind of Fully Convolutional Network (FCN) (Long et al., 2015), as it has high accuracy in pixel-by-pixel detection. Additionally, Ronneberger et al. (2015) showed, this network has a high efficacy when trained with a small image set, as the case of medical images databases, combined with a data augmentation process. In this work, authors utilized ResNet50 as a trained model and transfer learning with weights from ImageNet (Deng et al., 2009). Figure 4 shows samples of images used for training dataset, corresponding to patch images containing MAs, which may vary from having one single MA or multiple MAs.

In order to increase the number of training images and, consequently, having a model with an increased robustness, authors utilized a data augmentation process. This process consists in applying random rotations, random reductions, vertical and horizontal flips and random affine transformations. The magnitude of each of these transformations is also applied randomly, which allowed to increase by a factor of 5 the training dataset. Figure 5 presents a sample image of the resulting data augmentation.

False Positives Removal

It is certain that for medical applications, instead of removing false positives, it is essential to beware of false negatives, as the latter means disregarding the presence of the disease. However, for results obtained by U-Net, it turns out more suited to make a false positive removal, as results mostly show

Figure 3. Stages of fundus image pre-processing: Original (top), gamma correction (center) and CLAHE (bottom)

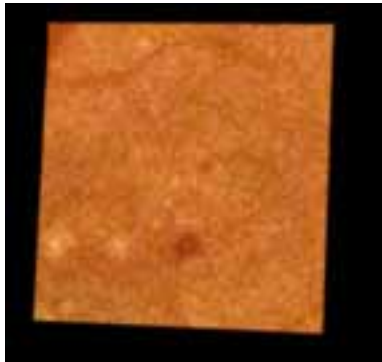


Figure 4. Sample patch images used in U-Net training showing presence of one single MA, multiple MAs, and their respective correct segmentation



a greater number of MAs than the actual number of MAs in the ground-truth. Moreover, based on the certitude that only one MA is enough evidence of DR presence, for images with a large amount of MAs, even when some MAs could be inevitably missed, it is not foreseen that this affects the diagnosis. Nevertheless, this is the reason why it is considered that the performance of this proposal is more significant in cases with a small number of MAs.

Figure 5. Sample patch image for training obtained from data augmentation

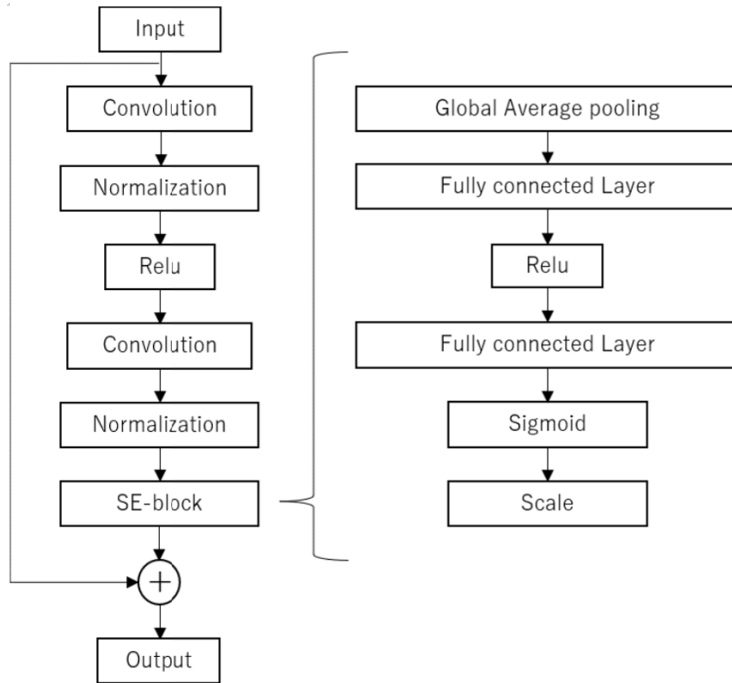


Therefore, a classifier was created to determine for each patch that firstly was detected as containing MAs, whether it really contains MAs or not. The classifier input corresponds to patch images where MAs were detected by U-Net. As the number of features that can clearly determine a MA is very small, it is necessary to extract features by a CNN. However, if the layers are made deeper to extract advanced and complex features, the performance becomes worse due to the gradient vanishing problem (He et al., 2016). As false positive removal is a crucial step for increasing the evaluation metrics and effectiveness of the proposal, diverse models were created and tested for assessing their performance. Firstly, a basic 6 layered CNN based on input, convolution, pooling and output layers, was used to verify the effectiveness of ResNet architecture, consisting of more than 18 layers. Considering the fact that deeper layers allow the extraction of more complex features, authors attempted to achieve the same task by using ResNet50. In order to go one step further, two more approaches based on ResNet50 were tested. The first one consists of ResNet50 + FineTurning, which is a method used to update the model by relearning the weights of the feature extraction layer, as well as additional learning of the final output layer in the ResNet50 learning model. The second one consists of ResNet50 + SE-block, a block consisting of squeeze and excitation (SE). This block has the purpose of improving the quality of representations produced by a network by modelling the interdependencies between the channels of its convolutional features (Hu et al., 2018). Figure 6 shows the description of residual module of SE-ResNet. The input of the block is a convolutional block. Then, a single numeric value is obtained from the channels by using average pooling, which represents the squeezing part of the block. For adding non-linearity, dense layer followed by ReLU function are used. Subsequently, another dense layer followed by sigmoid function gives each channel a smooth gating function and, lastly, each feature map of the convolutional block is weighted based on the side network, which represents the excitation part. Finally, a false positive removal based on ResNet101 + FineTurning was employed. For each model, after the classification of each patch image, these are merged into a single result image.

EXPERIMENTAL RESULTS

In this section, authors demonstrate the efficacy of the proposed method on two public databases, namely IDRiD (Porwal et al., 2020) and E-ophtha (Decenci re et al. 2013). Firstly, the training results for both networks are introduced and partial results from U-Net segmentation are shown. Finally, authors evaluate the performance of methodology and display final results. Additionally, authors present a quantitative comparison with MAs detection related works.

Figure 6. Residual module of SE-ResNet



Datasets

In this study, authors use two fundus image databases, namely IDRiD and E-ophtha (Decencièrè et al. 2013), which are widely used databases for lesion detection tasks. IDRiD database consists of 54 images for training and 27 images for test. Regarding E-ophtha database, it consists of 383 fundus images. Samples of these datasets are shown in Figure 7. Furthermore, for each image in both databases, it is provided its respective binary image that represents the accurate MAs segmentation done by a doctor.

Authors used IDRiD database for ResNet training. From the 54 images for training 2000 patch images containing MAs and patch images with no MAs are extracted. From this set, authors used 1600 images for training and 400 for validation. All images were labeled for training as “MA” and “No MA”. Based on the size of MAs, the patch images size was set to 128×128 pixels.

Network Training

For MAs detection authors used U-Net architecture. After training, this network reached approximately 0.35 and 0.50 for training loss and validation loss, respectively. While Intersection over Union (IoU), a metric used to assess the accuracy of algorithms for object detection, equal to the quotient of the intersection area of the predicted result and the ground truth, roughly approached to 0.50 and 0.35 for training and validation, respectively. This performance is not suitable, especially for medical field applications, where high sensitivity and specificity are crucial for the diagnosis of patients. As shown in Figure 8, segmentation results obtained by U-Net included patch images with exclusively true positives, patch images entirely with false positives, and patch images with presence of both true positives and false positives. This motivated the authors to create a second network to serve as a patch image classifier.

Figure 7. Sample images from databases IDRiD (top) and E-optha (bottom)

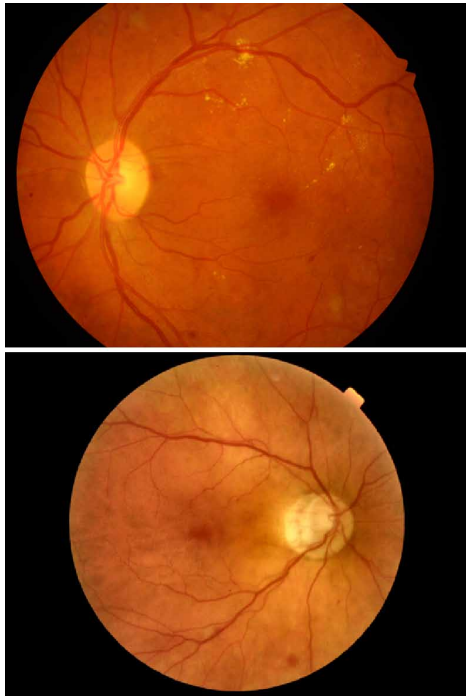
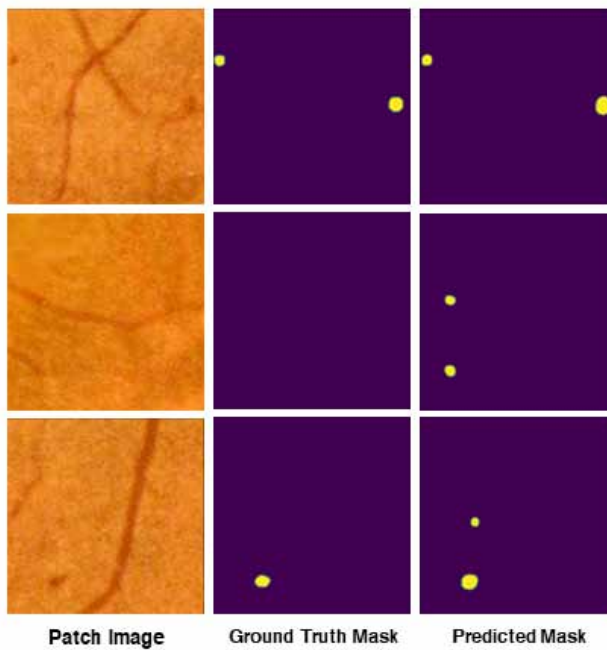


Figure 8. Fundus patch image, correct segmentation and result obtained in U-Net for MAs detection. Results show different segmentations that include exclusively true positives (first row), false positives (second row) and presence of both (third row)



The patch classification task was tested using five different models. For each of these, the loss function and accuracy obtained during the training process is shown in Figure 9. It is noticeable that the most basic 6 layered CNN does not achieve a favorable result, as the accuracy converged to about 65%. Concerning ResNet50, the accuracy did not improve much compared to the previous model. However, when FineTurning is included in the training process, the accuracy is greatly improved to about 95% for training data and about 75% for validation data. On the other hand, SE-block did not improve the accuracy. Finally, ResNet101 + FineTurning showed a slight improvement. Results suggest that ResNet101 + FineTurning is effective in removing false positives for this application, reaching an accuracy of 95% for training and 80% for validation and, therefore, this is the model used in the final approach for MAs segmentation.

Performance on Public Databases IDRiD and E-opththa

Authors used area under precision-recall curve (AUPR) as evaluation metric. The reason for this is that AUPR is a more representative metric for the lesion segmentation performance when compared to Receiver Operating Characteristic (ROC) curve and, additionally, AUPR is more realistic when dealing with skewed datasets (Porwal et al., 2020; Davis & Goadrich, 2006). For the purpose of evaluating the work, authors consider as true positive MA segmentation a result that is partially overlapped over the ground-truth, while false negative refers to a MA that was mistakenly not detected. False positive involves to indicating presence of a MA when it was not present over that region.

An example of the performance of the proposed method for IDRiD and E-opththa databases is shown in Figure 10. It results evident that the proposal results are favorable for both databases. Moreover, a summary of different fundus images corresponding to both datasets is shown in Table 1. Results for some images present a perfect performance in MAs detection (e.g. E-opththa4, E-opththa11, E-opththa17 and E-opththa21), while results in some others have an inferior performance (e.g. IDRiD 57, E-opththa5 and E-opththa12).

Recognizing the origin causing this difference in performance between images led the authors to search for a pattern existing in the presence of wrong segmentation results. Concerning false positives, there is a perceptible tendency that these appear over blood vessels. Indeed, from Table 1, false positives situated over blood vessels represent 75% of the total false positives. Examples of this pattern existing over blood vessels are shown in Figure 11. As mentioned previously, similarities between blood vessels and MAs exist, which complicates the distinction of these two when they are overlapped and, as a consequence, this affects the performance of the algorithm for MAs detection.

Nonetheless, even if there is a propensity for false positives, regarding false negatives, there is not a clear pattern for their presence. While some of them are located over blood vessels, the proportion is

Figure 9. Loss function and accuracy for training process for models used for false positive removal: six layered CNN (first column), ResNet50 (second column), ResNet50+FineTurning (third column), ResNet50+SE-block (fourth column) and ResNet101+FineTurning (fifth column)

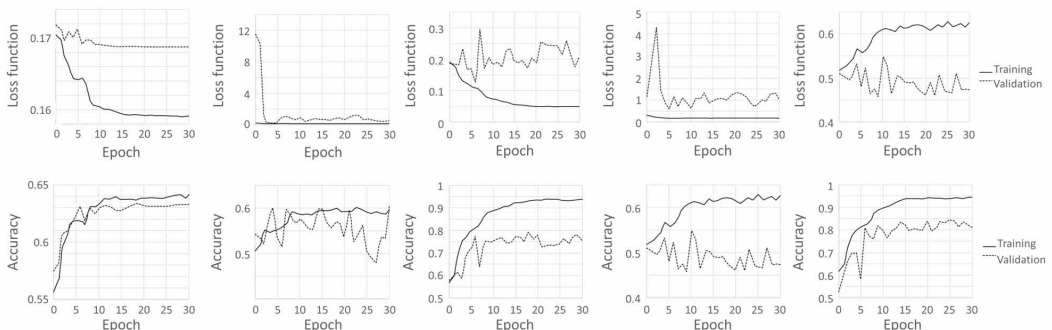


Figure 10. An example of MAs detection results. First row shows sample result obtained for IDRiD database while second row for E-ophtha database. Original images are shown in first column, their respective ground-truth for MAs is found in the second column, and segmentation result with the proposed method is displayed in third column, where red and white pixels represent true positives and false positives, respectively

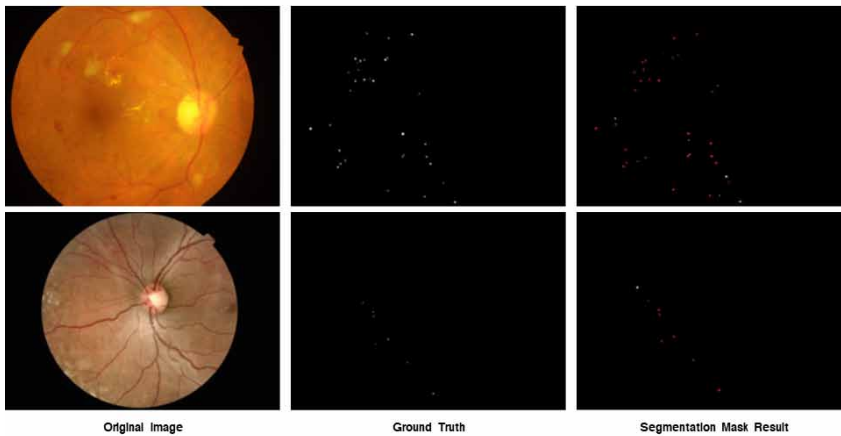


Table 1. MAs detection results for sample images from IDRiD and E-ophtha databases

Image	Ground Truth	Number of Detections	True Positives	False Positives	False Negatives	Recall	Precision Ratio
IDRiD63	3	2	2	0	1	0.667	1.000
IDRiD80	4	3	3	0	1	0.750	1.000
IDRiD57	10	8	6	2	4	0.600	0.750
E-ophtha17	3	3	3	0	0	1.000	1.000
E-ophtha11	4	4	4	0	0	1.000	1.000
E-ophtha22	4	6	4	2	0	1.000	0.667
E-ophtha12	5	8	5	3	0	1.000	0.625
E-ophtha21	5	5	5	0	0	1.000	1.000
E-ophtha4	6	6	6	0	0	1.000	1.000
E-ophtha5	6	5	4	1	2	0.667	0.800

not as meaningful as for false positives. Figure 12 shows a pair of false negatives for cases presented over a blood vessel and other region.

While IDRiD and E-ophtha databases present fundus images with a number of MAs ranging from one to more than ninety, on Table 1 authors focused on showing the performance for those images with presence of less than ten MAs. The reason for this is that the main objective is the detection of MAs in early stages, when only few MAs are present and irreversible damage caused by DR can be prevented. Additionally, it is possible to assume that it is more complicated for physicians to distinguish an unhealthy fundus when the number of MAs is lower, hence a method with efficacy for those cases is more reliable for assisting in the evaluation of fundus images.

Authors present a comparison of lesion segmentation including MAs for IDRiD dataset by various models (Porwal et al., 2020; Wan et al., 2021). Table 2 shows AUPR results for MAs segmentation for these models in IDRiD database and results of the proposed method for both IDRiD and E-ophtha

Figure 11. False positive samples present in Segmentation Mask Result for E-ophtha22 (first row), E-ophtha12 (second row) and IDRiD57 (third row)

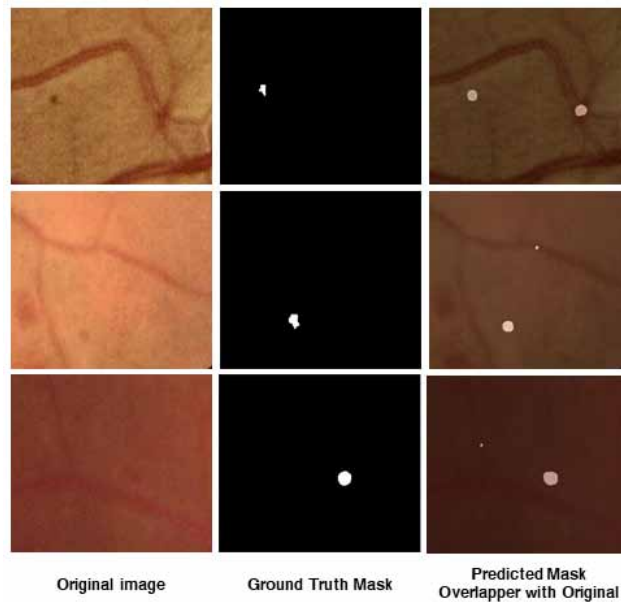
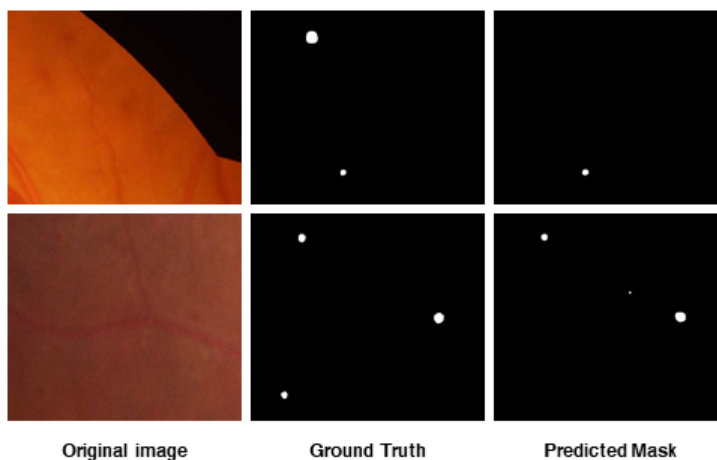


Figure 12. False negative samples present over blood vessel in IDRiD63 (first row) and over a no blood vessel related region in IDRiD57 (second row)



databases. The related works belong to the top 4 teams for MAs lesion segmentation. The employed methods vary significantly from one to another. iFLYTEK uses Cascade CNN, standing for the usage of multiple CNN in the process. Similarly, PATech team also adopted an ensemble strategy, by using DenseNet, a type of CNN with the so called Dense Blocks, where all layers are directly connected with each other. PATech team used this architecture together with U-Net, which was previously described in this paper. Regarding to the teams that utilized one single architecture, VRT team proposal solely used U-Net for segmentation, while SDNU team utilized Mask R-CNN, a type of CNN based on analyzing regions of interest obtained from several regions of the image. These teams also made use

Table 2. Comparison of AUPR for MAs detection teams and their respective approach

Team Name and database	Approach	AUPR
iFLYTEK (IDRiD)	Cascaded CNN	0.5017
VRT (IDRiD)	U-Net	0.4951
PATech (IDRiD)	DenseNet + U-Net	0.4740
SDNU (IDRiD)	Mask R-CNN	0.4111
Proposed method (IDRiD)	U-Net + ResNet101	0.5254
Proposed method (E-ophtha)	U-Net + ResNet101	0.5411

of data augmentation, which include diverse image transformations such as flips, rotations, scalings, translations, crops, shearings, and color transformations.

The significance of this proposal lies in the addition of ResNet as a false positive remover, which allowed to improve the results in MAs detection. This is reflected in the AUPR results for MAs detection for both databases. For IDRiD database, AUPR passed from 0.39 to 0.5254 with ResNet, while for E-ophtha database it passed from 0.4007 to 0.5411. The results shown in Table 2 indicate that the proposed method outperforms previous works in AUPR, including other ensemble approaches, meaning that in comparison, this method is capable to detect most of the MA without making many false positive detections in more than one database, making it a more robust method for MAs detection.

CONCLUSION

This paper presents an efficient method for segmentation of MAs in fundus images. Authors base their method in two different networks: U-Net and ResNet. Firstly, authors apply contrast enhancement to the fundus image. Then, fundus patch images are passed to U-Net, which performs MAs segmentation. As results obtained in segmentation include several false positives, a second network based on ResNet101 with FineTuning is used to remove false positive patches. After false positives removal, all the patches are merged to obtain one single image representing the positions of MAs in fundus.

Due to the similarity of MAs with blood vessels and the low contrast between MAs and background, MAs segmentation is a challenging task even for physicians. These causes are the essential complication for MAs detection. For this reason, authors avoided methods primarily based on image processing, and the approach works based on deep learning for segmentation, which allows to extract more complex features.

Databases used in experiments have a mostly uniform illumination. In order to make a more robust system, authors plan to test the method on fundus images with different lighting conditions, and depending on the results, trying different strategies to solve this issue. Authors foresee to extend this methodology to wide-angle fundus images and, in this way, making a more extensive and complete diagnosis.

REFERENCES

- Bhatia, K., Arora, S., & Tomar, R. (2016, October). Diagnosis of diabetic retinopathy using machine learning classification algorithm. In *2016 2nd international conference on next generation computing technologies (NGCT)* (pp. 347-351). IEEE.
- Davis, J., & Goadrich, M. (2006, June). The relationship between Precision-Recall and ROC curves. In *Proceedings of the 23rd international conference on Machine learning* (pp. 233-240). Association for Computing Machinery. doi:10.1145/1143844.1143874
- Decencière, E., Cazuguel, G., Zhang, X., Thibault, G., Klein, J.-C., Meyer, F., Marcotegui, B., Quéllec, G., Lamard, M., Danno, R., Elie, D., Massin, P., Viktor, Z., Erginay, A., Laÿ, B., & Chabouis, A. (2013). TeleOphta: Machine learning and image processing methods for teleophthalmology. *IRBM*, *34*(2), 196–203. doi:10.1016/j.irbm.2013.01.010
- Deng, J., Dong, W., Socher, R., Li, L.-J., Li, K., & Fei-Fei, L. (2009). Imagenet: A large-scale hierarchical image database. In *Conference on computer vision and pattern recognition* (pp. 248–255). IEEE. doi:10.1109/CVPR.2009.5206848
- Eftekhari, N., Pourreza, H. R., Masoudi, M., Ghiasi-Shirazi, K., & Saeedi, E. (2019). Microaneurysm detection in fundus images using a two-step convolutional neural network. *Biomedical Engineering Online*, *18*(1), 1–16. doi:10.1186/s12938-019-0675-9 PMID:31142335
- He, K., Zhang, X., Ren, S., & Sun, J. (2016). Deep residual learning for image recognition. In *Proceedings of the conference on computer vision and pattern recognition* (pp. 770-778). IEEE.
- Hu, J., Shen, L., & Sun, G. (2018). Squeeze-and-excitation networks. In *Proceedings of the conference on computer vision and pattern recognition* (pp. 7132-7141). IEEE.
- Jiang, H., Yang, K., Gao, M., Zhang, D., Ma, H., & Qian, W. (2019, July). An interpretable ensemble deep learning model for diabetic retinopathy disease classification. In *2019 41st annual international conference of the engineering in medicine and biology society (EMBC)* (pp. 2045-2048). IEEE.
- Joshi, S., & Karule, P. T. (2020). Mathematical morphology for microaneurysm detection in fundus images. *European Journal of Ophthalmology*, *30*(5), 1135–1142. doi:10.1177/1120672119843021 PMID:31018679
- Kumar, S., & Kumar, B. (2018, February). Diabetic retinopathy detection by extracting area and number of microaneurysm from colour fundus image. In *5th International Conference on Signal Processing and Integrated Networks (SPIN)* (pp. 359-364). IEEE.
- Long, J., Shelhamer, E., & Darrell, T. (2015). Fully convolutional networks for semantic segmentation. In *Proceedings of the conference on computer vision and pattern recognition* (pp. 3431-3440). IEEE.
- Mahendran, G., & Dhanasekaran, R. (2015). Investigation of the severity level of diabetic retinopathy using supervised classifier algorithms. *Computers & Electrical Engineering*, *45*, 312–323. doi:10.1016/j.compeleceng.2015.01.013
- Manohar, P., & Singh, V. (2018, February). Morphological approach for Retinal Microaneurysm detection. In *Second International Conference on Advances in Electronics, Computers and Communications (ICA ECC)* (pp. 1-7). IEEE.
- Miyashita, M., Hatanaka, Y., Ogohara, K., Muramatsu, C., Sunayama, W., & Fujita, H. (2018). Automatic detection of microaneurysms in retinal image by using convolutional neural network. *Med Imaging Technol*, *36*(4), 189–195.
- Pizer, S. M., Amburn, E. P., Austin, J. D., Cromartie, R., Geselowitz, A., Greer, T., Romeny, B. T. H., Zimmerman, J. B., & Zuiderveld, K. (1987). Adaptive histogram equalization and its variations. *Computer Vision Graphics and Image Processing*, *39*(3), 355–368. doi:10.1016/S0734-189X(87)80186-X
- Porwal, P., Pachade, S., Kokare, M., Deshmukh, G., Son, J., Bae, W., Liu, L., Wang, J., Liu, X., Gao, L., Wu, T. B., Xiao, J., Wang, F., Yin, B., Wang, Y., Danala, G., He, L., Choi, Y. H., Lee, Y. C., & Meriaudeau, F. (2020). Idrid: Diabetic retinopathy–segmentation and grading challenge. *Medical Image Analysis*, *59*, 101561. doi:10.1016/j.media.2019.101561 PMID:31671320

Ronneberger, O., Fischer, P., & Brox, T. (2015, October). U-net: Convolutional networks for biomedical image segmentation. In *International Conference on Medical image computing and computer-assisted intervention* (pp. 234-241). Springer. doi:10.1007/978-3-319-24574-4_28

Sarhan, M. H., Albarqouni, S., Yigitsoy, M., Navab, N., & Eslami, A. (2019, October). Multi-scale microaneurysms segmentation using embedding triplet loss. In *International Conference on Medical Image Computing and Computer-Assisted Intervention* (pp. 174-182). Springer. doi:10.1007/978-3-030-32239-7_20

Selcuk, T., & Alkan, A. (2019). Detection of microaneurysms using ant colony algorithm in the early diagnosis of diabetic retinopathy. *Medical Hypotheses*, 129, 109242. doi:10.1016/j.mehy.2019.109242 PMID:31371092

Wan, C., Chen, Y., Li, H., Zheng, B., Chen, N., Yang, W., Wang, C., & Li, Y. (2021). EAD-net: A novel lesion segmentation method in diabetic retinopathy using neural networks. *Disease Markers*, 2021, 2021. doi:10.1155/2021/6482665 PMID:34512815

Yahui Peng received the B.E. degree in Engineering Physics from Tsinghua University, Beijing, China, in 1998, the M.E. degree in Nuclear Technology and Applications from Tsinghua University, Beijing, China, in 2001, and the Ph.D. degree in Medical Physics from the University of Chicago, Chicago, IL, USA, in 2010. Currently, he is a full Professor affiliated with the School of Electronic and Information Engineering at Beijing Jiaotong University, Beijing, China. He has extensive research experience in computer-aided diagnosis of prostate cancer in MR images, supported by grants from National Institutes of Health, Department of Defense and Natural Science Foundation of China. He has published more 50 peer-reviewed journal papers.